

## Communications

### Synthesis and Properties of Phase Change Material-Polypyrrole Core-Shell Nanocapsules *via* Fe<sup>3+</sup>-Oxidative Miniemulsion Polymerization

Hyun Woog Ryu<sup>1</sup>, Sang Phil Park<sup>1</sup>, Seung Mo Lee<sup>1</sup>, Sun Jong Lee<sup>1</sup>, Won-Gun Koh<sup>1</sup>, In Woo Cheong<sup>2</sup>, and Jung Hyun Kim<sup>\*1</sup>

<sup>1</sup>Nanosphere Process and Technology Laboratory, Department of Chemical Engineering, Yonsei University, Seoul 120-749, Korea

<sup>2</sup>Department of Applied Chemistry, Kyungpook National University, Daegu 702-701, Korea

Received November 14, 2012; Revised February 11, 2013;  
Accepted February 13, 2013

#### Introduction

Phase change materials (PCMs) are one of the most important functional materials that can absorb, store, and release large amounts of latent heat over a defined temperature range when undergoing phase or state changes, and have attracted great attention from both scientific and industrial communities.<sup>1-3</sup> The bulk PCMs cannot easy to handle in practical application because of the supercooling problem and interfacial combination with the circumstance materials, although they can provide high latent heat. Encapsulation of functionally active materials in hollow microspheres is an attractive way of storing. It can protect these active materials from reaction towards the outside environment when required for fulfilling appropriate applications. Therefore this method may offer a solution to these problematic limitations.

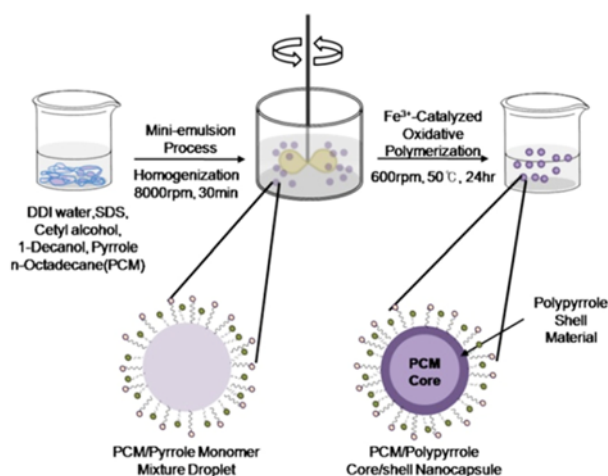
Polypyrrole (PPy) is not only an important component of conjugated polymers due to its usability in a wide range of applications, but also one of the most studied conducting polymers because of its higher conductivity and better environmental stability in the conductive (oxidative) state than any other conducting polymer. PPy can be easily prepared by chemical oxidative and electrochemical polymerization. In a chemical oxidative polymerization, (NH<sub>4</sub>)<sub>2</sub>S<sub>2</sub>O<sub>8</sub>, H<sub>2</sub>O<sub>2</sub>, and many kinds of salts containing transition metal ions,

*e.g.*, FeCl<sub>3</sub> or CuCl<sub>2</sub>, are generally used as oxidants. It is important to improve the process ability, conductivity, and environmental stability of PPy for the wide range of applications in various fields.<sup>4</sup>

PCMs have been synthesized using *n*-octadecane as a core and polyurea as a shell by many researchers.<sup>5-7</sup> The techniques used to synthesize the PCMs, however, have significant drawbacks of being expensive, time-consuming due to the multi-step procedure and low electrical or thermal conductivities. To best of our knowledge, there were no reports on the synthesis of PCM-PPy core-shell nanocapsules by Fe<sup>3+</sup>-catalyzed oxidative polymerization in the literature.<sup>8</sup> In this work, we have proposed a facile method for preparing PCM-PPy core-shell nanocapsules *via* Fe<sup>3+</sup>-oxidative polymerization in miniemulsion system. This facile method includes a FeCl<sub>3</sub>/H<sub>2</sub>O<sub>2</sub> (catalyst/oxidant) combination system as oxidants.

#### Results and Discussion

A scheme for the formation of PCM-PPy core-shell nanocapsules is given in Scheme I. The fabrication was performed by Fe<sup>3+</sup>-catalyzed oxidative polymerization in miniemulsion system.<sup>9</sup> In this polymerization, long chain alkane or alcohol is usually used as the hydrophobic material. The PCM (*n*-octadecane) used in this work is a long chain alkane, which was utilized as hydrophobic core material. The PCM-PPy droplets and cetyl alcohol were dispersed in an aqueous medium under vigorous agitation. Other water-soluble components, such as sodium dodecyl sulfate (SDS), 1-dodecanol, H<sub>2</sub>O<sub>2</sub> and FeCl<sub>3</sub> are dissolved in the aqueous phase. Pyrrole (Py) monomer of PCM-PPy core-shell droplets was polymerized by the Fe<sup>3+</sup>-catalyzed oxidative polymerization in



**Scheme I.** A schematic illustration for the preparation of PCM-PPy nanocapsules.

\*Corresponding Author. E-mail: jayhkim@yonsei.ac.kr

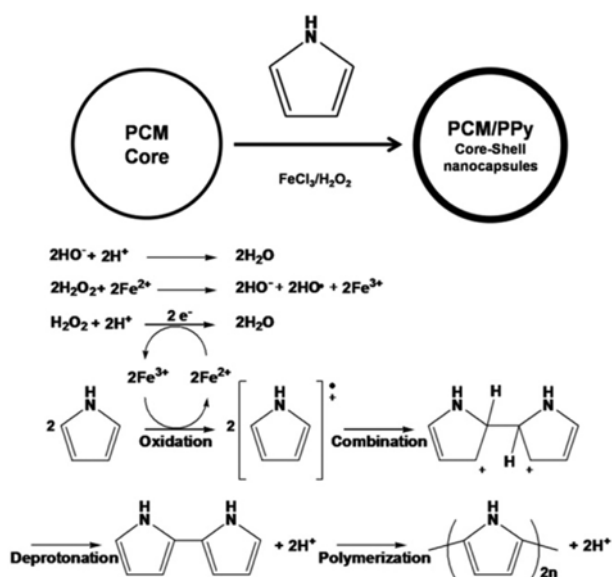


**Figure 1.** Detailed reaction mechanism of PCM-PPy nanocapsules via  $\text{Fe}^{3+}$ -catalyzed oxidative polymerization.

the aqueous medium.

Figure 1 shows a proposed mechanism for the  $\text{Fe}^{3+}$ -catalyzed oxidative polymerization of Py during the formation of PPy shell. As polymerization proceeds, Py oligomer chains continue to grow up by the oxidation reaction with  $\text{Fe}^{3+}$  at the surface of pre-existing droplets and consequently, PPy becomes the shell of the core-shell nanocapsules. Meanwhile,  $\text{Fe}^{2+}$  ions are regenerated by  $\text{H}_2\text{O}_2$  and the shell is replenished by diffusing Py monomers from the inner-core phase. During the polymerization, the oxidative polymerization takes place at the nanocapsule surface. The enrichment of  $\text{Fe}^{3+}$  ions at the capsule surface can be rationalized by the ionic attraction between sulfate ( $\text{OSO}_3^-$ ) groups and  $\text{Fe}^{3+}$  ions. Eventually, PPy gradually solidifies on the shell portion and become hard shell. Consequently, PCM-PPy core shell nanocapsules can be successfully formed.<sup>4,10,11</sup>

We present scanning electron microscopy (SEM) and transmission electron microscopy (TEM) images of the PCM-PPy microcapsules prepared by using  $\text{Fe}^{3+}$ -catalyzed oxidative miniemulsion polymerization in Figure 2(a)-(d). In the preparation, PCM was varied from 10 to 40 wt% per Py monomer. All samples showed more than 95% Py conversion, measured by gravimetric method. The PCM-PPy nanocapsules had spherical morphology and they were well dispersed in aqueous medium. The TEM images for corresponding samples were illustrated in each SEM image. As shown in the insets of Figure 2(a)-(d), the shell and core parts of the nanocapsules show different contrast, confirming core-shell morphology. The proportion of encapsulated PCM has an effect on nanocapsules size. Gradually inner PCM was increased PCM-PPy core-shell nanocapsules was bigger than few ratio PCM samples. This is due to the presence of PCM core

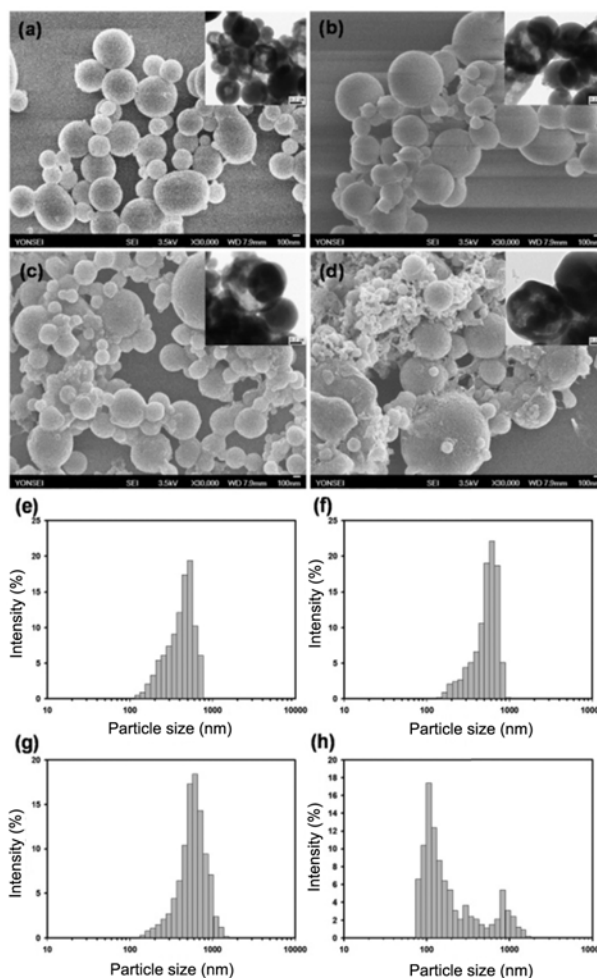


**Figure 2.** SEM and TEM (inlet) images of PCM-PPy nanocapsules prepared with ratio control of PCM weight percent. PCM ratio (per Py monomer) and particle size of the PCM-PPy nanocapsules: (a) 10 wt%, 830 nm; (b) 20 wt%, 912 nm; (c) 30 wt%, 950 nm; and (d) 40 wt%, 1150 nm. (e-h) each was particle size distribution.

material in the core part of the PCM-PPy core-shell nanocapsules. Figure 2(e) the particle size distributions of the PCM-PPy nanocapsules seem quite broad. The number average sizes of the individual PCM-PPy core-shell nanocapsules significantly increased from 470 to 1150 nm.

In order to confirm core/shell morphology of the nanocapsules, *n*-octadecane in core part was extracted by using petroleum ether prior to SEM analysis and the SEM images were illustrated in Figure 3. As shown in Figure 3(a)-(d), the nanoparticles shriveled as a result of empty cores (*n*-octadecane) and thin sheath (PPy).

Figure 4 shows DSC curves of the PCM-PPy core-shell nanocapsules upon heating/cooling cycles. Energy storage/release capacities of the PCM-PPy core-shell nanocapsules and encapsulation efficiency were calculated by DSC analysis program. The integration of DSC curve for PCM 30% sam-

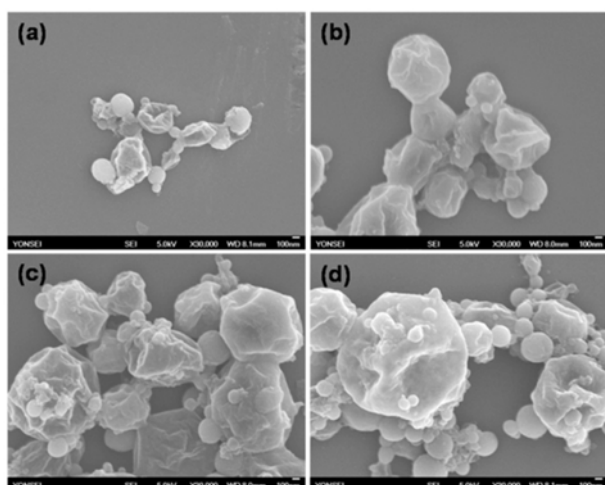


**Figure 3.** SEM images of PCM-PPy nanocapsule sheaths after dissolution in petroleum ether.

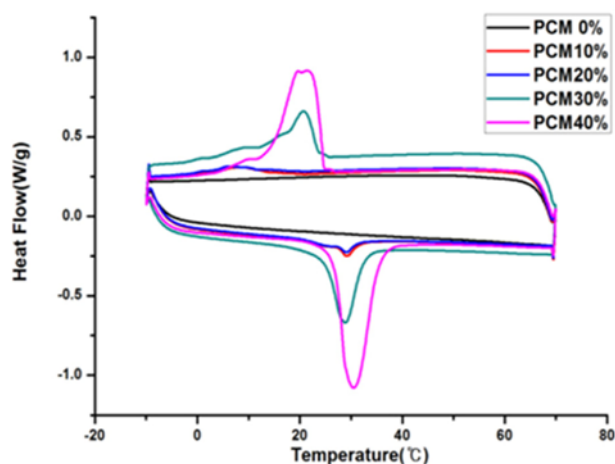


**Figure 4.** DSC curves of PCM-PPy core-shell nanocapsules.

ple upon heating from 10 to 150 °C at two cycles revealed that the latent heat of PCM-PPy nanocapsules are approximately 33.3 J/g (usually, this should indicate crystallization enthalpy).

The encapsulation efficiency (% EE) of the PCM-PPy nanocapsules is expressed as:

$$EE (\%) = \frac{\Delta H_c}{\frac{W_o}{W_s} \times \Delta H_o} \times 100 (\%) \quad (1)$$

Where  $\Delta H_c$  is the crystallization enthalpy of nanocapsules,  $\Delta H_o$  is the crystallization enthalpy of pure *n*-octadecane,  $W_o$  is the weight of *n*-octadecane encapsulated,  $W_s$  is the weights of *n*-octadecane and Py monomer in the feed. The EE and  $\Delta H_c$  of the nanocapsules were 2.84%, 4.2 J/g at 10 wt% of PCM, 10.64%, 5.31 J/g at 20 wt% of PCM and 34.7%, 14.83 J/g at 30 wt% of PCM, respectively. The EE values of PCM-PPy nanocapsules were summarized in Table I. The EE and

**Table I.** Encapsulation Efficiency of the PCM-PPy Nanocapsules

PCM Weight Percent per Pyrrole (wt%)	Encapsulation Efficiency (%)
10	2.87
20	10.64
30	30.83
40	23.59

$\Delta H_c$  of the nanocapsules were increased with increase of amount the PCM weight from 10 to 30 wt%.<sup>12,13</sup> The results would imply that the colloidal stability of PCM-Py droplets was maintained during the oxidative polymerization up to 30 wt% of PCM. The factors that would be noticeable can be thermodynamic aspect concerned with interfacial tension between PCM and shell polymer. Interfacial tension between oil droplets and water phase is reduced during polymerization.<sup>14</sup> Therefore, the polymer can be separated from the oil droplet containing PCM. The possibility of encapsulation has been predicted from spreading coefficients and interfacial tensions.

Regarding electrical conductivity of the nanocapsules, sheet resistance ( $\Omega/\text{sq}$ ) was measured by using standard four-point probe technique at 20 °C. As seen in the Figure 5, sheet resistance of the PCM-PPy nanocapsules slightly increased as PCM proportion increased from 0 to 30 wt%, *i.e.*, the larger amount of PCM in the PCM-PPy nanocapsules resulted in the higher sheet resistance of the PCM-PPy nanocapsules. When the content of the PCM was increased from 10 to 30 wt%, the encapsulation efficiency was also increased. However, PCM 40 wt% or more in the presence of excess of PCM does not go to the core of the nanocapsules. Excess PCM acts as a kind of insulator between nanocapsule. When the PCM weight percent was 40 wt% more, sheet resistance also

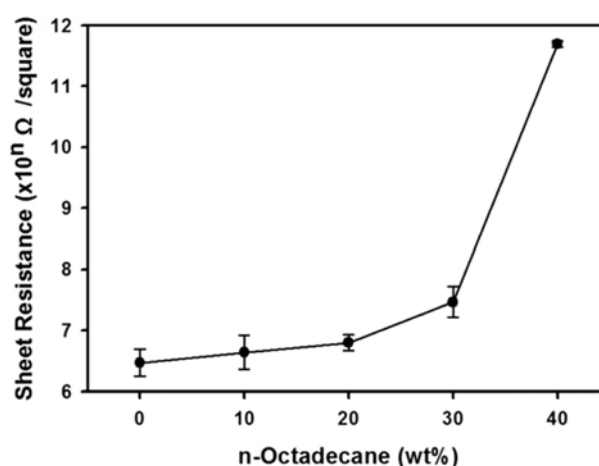


**Figure 5.** The sheet resistance of PCM-PPy nanocapsules controlled by PCM ratio control.

dramatically increased. It showed that PCM was not completely encapsulated and was located on the PCM-PPy nanocapsules surface and caused increased sheet resistance. When the PCM weight percent was 0, 10, 20, 30 and 40%, the sheet resistivity of the corresponding PCM-PPy core shell nanocapsules was  $3.4 \times 10^6$ ,  $6.9 \times 10^6$ ,  $8.6 \times 10^6$ ,  $4.7 \times 10^7$ , and  $7.1 \times 10^{11}$   $\Omega/\text{sq}$ , respectively.

In summary, we demonstrated that the PCM-PPy core-shell nanocapsules were successfully prepared by using Fe<sup>3+</sup>-catalyzed oxidative polymerization by miniemulsion process in aqueous medium. The morphology of particle was confirmed by SEM and TEM analyses. The particle size distribution and the heat capacity of PCM-PPy nanoparticle were analyzed by DLS and DSC, respectively. When the concentration of PCM core material was increased from 10 to 30 wt%, the encapsulation efficiency of the PCM-PPy nanoparticles was increased, but it was decreased when it was 40 wt% and above. The sheet resistivity of HCl-doped nanocapsules was  $10^7$   $\Omega/\text{sq}$  at 30 wt% PCM concentration. This new strategy is universal for the synthesis of many other conjugated materials and this approach suggests a new synthetic direction for the PCM-conducting polymer core-shell nanocapsules by oxidative miniemulsion polymerization.

**Acknowledgments.** This work was supported by the National Research Foundation (NRF) grant funded by the Korea government (MEST) through the Active Polymer Center for Pattern Integration (No. R11-2007-050-00000-0) and a grant from the Industrial Technology Development program (K0006005) of the Ministry of Knowledge Economy (MKE) of Korea. This research was supported by NanoMaterial Technology Development Program through the National Research Foundation of Korea (NRF) funded by the Ministry of Education, Science

and Technology (2008-2002380/2012-0006227). The research was supported by the Pioneer Research Center Program through the National Research Foundation of Korea funded by the Ministry of Education, Science and Technology (No. 2010-0019308/2012-0000424). This research was also supported by the Converging Center Program through the Ministry of Education, Science and Technology (2010K001430).

## References

- (1) A. Abhat, *Solar Energy*, **30**, 313 (1983).
- (2) N. Bechthold, F. Tiarks, M. Willert, K. Landfester, and M. Antonietti, *Macromol. Symp.*, **151**, 549 (2000).
- (3) B. Zalba, J. M. Marín, L. F. Cabeza, and H. Mehling, *Appl. Ther. Eng.*, **23**, 251 (2003).
- (4) J. M. Lee, D. G. Lee, S. J. Lee, J. H. Kim, and I. W. Cheong, *Macromolecules*, **42**, 4511 (2009).
- (5) H. Zhang and X. Wang, *Sol. Energy Mater. Sol. Cells*, **93**, 1366 (2009).
- (6) N. Sarier and E. Onder, *Thermochim. Acta.*, **454**, 90 (2007).
- (7) M. You, X. Zhang, W. Li, and X. Wang, *Thermochim. Acta*, **472**, 20 (2008).
- (8) S. J. Lee, J. M. Lee, I. W. Cheong, H. Lee, and J. H. Kim, *J. Polym. Sci. Part A: Polym. Chem.*, **46**, 2097 (2008).
- (9) A. J. P. van Zyl, D. Wet-Roos, R. D. Sanderson, and B. Klumperman, *Eur. Polym. J.*, **40**, 2717 (2004).
- (10) S. J. Lee, J. M. Lee, H.-Z. Cho, W. G. Koh, I. W. Cheong, and J. H. Kim, *Macromolecules*, **43**, 2484 (2010).
- (11) Y. J. Jung, S. J. Lee, S. W. Choi, and J. H. Kim, *J. Polym. Sci. Part A: Polym. Chem.*, **46**, 5968 (2008).
- (12) S. Torza and S. Mason, *J. Colloid Interface Sci.*, **33**, 67 (1970).
- (13) Y. Luo and X. Zhou, *J. Polym. Sci. Part A: Polym. Chem.*, **42**, 2145 (2004).
- (14) M. Hawlader, M. Uddin, and M. M. Khin, *Appl. Energy*, **74**, 195 (2003).